Enhancing interpretability of seismic data with spectral decomposition phase components

Satinder Chopra[+] and Kurt J. Marfurt[†]*
[+]Arcis Seismic Solutions, TGS, Calgary; [†]The University of Oklahoma, Norman

Summary

Stratigraphic interpretation of seismic data requires careful interpretation of the amplitude, phase and frequency so as to gauge the geologic subsurface detail. Sometimes the interpretation of the changes in amplitudes is not easy and the equivalent phase is difficult to comprehend. In such cases seismic attributes are utilized to provide additional information that could aid the interpretation. One of the earliest set of 'instantaneous' attributes was based on complex trace analysis, and instantaneous phase has been used for interpretation of stratigraphic features such as pinchouts and discontinuities as well as fault edges.

In this study, we demonstrate that the interpretability of seismic data can be enhanced with the use of spectral phase components derived during spectral decomposition. As there are different methods for decomposing seismic data into its component frequencies and phase within the seismic bandwidth, we consider two of the common methods in our analysis here, namely the continuous wavelet transform and the matching pursuit methods. We also show that the principal component analysis of spectral magnitude and phase components yields additional insight into the data. The first principal component 'churned' out of the phase components shows clarity in the features of interest and compares favourably with the discontinuity attributes commonly used for the purpose.

Introduction

The strength of seismic reflections carry subsurface information sensitive to absorption and scattering, propagation through fluids and complex interference patterns from stacked stratigraphy. Quantitative interpretation requires that the seismic amplitudes be as 'true' as possible, and are not contaminated with noise or other distortions of the acquisition process. In addition to its reflection strength, seismic events are characterized by their frequency and phase. Thin bed interference often increases the high frequency and decreases the low frequency components of the seismic wavelet. For adjacent reflectors having equal but opposite reflection coefficients, the peak amplitude occurs or "tunes" at the quarter wavelength frequency. This latter thin bed tuning phenomena also gives rise to a 90^0 change in phase. Linear increases and decreases in impedance that may be associated with upward fining or coarsening also give rise to a 90^0 phase change, as does the reflection from an interface between two units of equal impedance but a finite change in attenuation, or *1/Q*. While changes in reflection strength are easy to see, the recognition of such phase and frequency changes are subtle and more easily overlooked on large 3D seismic data volumes. Seismic attributes quantify such subtle changes.

One of the early set of attributes were based on complex trace analysis. Referred to as 'instantaneous' attributes and introduced by Taner et al. (1979), the instantaneous envelope (also called reflection strength), phase, and frequency attributes are available in every seismic interpretation software package. We focus on the phase attribute in this study.

Instantaneous phase is the phase associated with a point in time and is quite different from the phase as a function of frequency we talk about in Fourier analysis. It is a local measure of the reflectivity response about a given time sample. Derived as ATAN2(u^H,u) where u^H is the Hilbert transform of measured seismic data, u and ATAN2 denotes the arctangent that results in values between -180^0 and $+180^0$. Mathematically, it is convenient to write these two traces as a complex trace, $U=u+ju^H$, where j is the square root of -1. The instantaneous phase attribute is independent of the reflection amplitude, such that fault planes through low amplitude but high signal-to-noise areas of the data are more easily seen. For the same reason, instantaneous phase is useful in delineating pinchouts, angularities, discontinuities, thin-bed interference patterns and in picking sequence terminations. Phase displays have also been used to show change of phase often present at the end of bright spots.

Phase has a natural discontinuity at multiples of 180^o, so the plot of phase has a saw tooth appearance. Since -180^o and 180^o are the same angle, a colour wheel or a cyclical colour bar is normally used for phase displays. Using the coloured phase displays, the phase corresponding to each peak and trough of the real trace is assigned the same colour, so that any phase change can be followed from trace to trace. Such colour bars also help phase displays emphasize the continuity of events. The software for complex trace analysis and generation of the instantaneous attributes is available on most interactive interpretation commercial workstation software packages. We used this software to generate the instantaneous phase attribute for a 3D seismic volume from northern-central Alberta, Canada.

Phase analysis with spectral decomposition

The phase of the reflection events in the seismic data can also be studied with spectral decomposition where the seismic data is decomposed into a suite of spectral magnitude and phase components, within the bandwidth of the data. Partyka et al. (1999) were the first to decompose a target formation into its spectral magnitude and phase components using a short window discrete Fourier transform. Other methods for carrying out spectral decomposition include the continuous wavelet transform (CWT) (Sinha et al., 2005), the S-transform (Stockwell et al., 1996) and matching pursuit decomposition (MPD) (Mallat and Zhang, 1993). While the spectral magnitude values depend on the amplitude levels of the input data, the phase component values range from -180 to $+180^o$. An important aspect of spectral decomposition is that magnitude and phase spectra of the seismic data can be studied in a frequency-dependent way, such that the definition of the geologic subsurface features are visualized at different frequencies. The sharper definition of the features seen in the phase spectra improves their interpretability.

DOI http://dx.doi.org/10.1190/segam2015-5874263.1

The output from spectral decomposition is a suite of spectral magnitude and phase volumes at user-defined frequency increments, which can be overwhelming to interpret. For extracting information from the different attributes, and yet not prove to be taxing, different methods have been developed. One such dimensionality reduction tool is the principal component analysis which can churn through the different attributes and yield one or two attributes that convey the desired information (Chopra and Marfurt, 2014). We employ principal component analysis on spectral decomposition spectral magnitude and phase components extracted using the CWT and the MPD methods and compare the results.

The spectral decomposition of the input seismic data was carried out using the CWT and the MPD techniques. The CWT transform method used here has been briefly described in Chopra and Marfurt (2015). It uses orthogonal basis wavelets so as to decompose the seismic trace into individual frequency components. A Morlet wavelet was chosen as the mother wavelet, which uses a time window that varies with frequency. The MPD spectral decomposition method used here has been described by Liu and Marfurt (2005). It is an iterative process. At each iteration, the envelope of the analytic trace is computed and the maximum envelope value is detected. Next, a subset of all the envelope peaks along the trace are selected that exceed a user-defined parameter. Analytic Ricker or Morlet mother wavelets from a precomputed wavelet library are least squares fit to the analytic trace, subtracted and a new residual is generated. The complex spectral components of these wavelets are multiplied by the phase corresponding to the wavelet time and accumulated, and in the process the spectral components of the entire trace are generated. The iterations continue till the residual falls below a certain threshold value.

Both these methods were applied on a 3D seismic volume from northern-central Alberta, Canada. In Figure 1 we show a segment of a seismic section and its equivalent sections from the instantaneous phase (Figure 1a), spectral magnitude (Figure 1c) and the phase component (Figure 1d). Some vertical discontinuities in the middle of the section are seen on the instantaneous phase section, not so clearly seen on the spectral magnitude, but are very clearly delineated on the phase component section. The yellow horizon shown on the images is at a level close to 1700ms.

In Figure 2 we show a comparison of stratal slices from the spectral magnitude volumes generated using the CWT and MP algorithms at 40, 50, 60 and 70 Hz. Notice that the lineaments in the NW-SE direction (as indicated with the pink arrows) are seen more clearly on the MP spectral displays than the equivalent CWT displays. There are some smaller E-W lineaments that are seen on these displays. In Figure 3 we show a comparison of phantom horizon slices 8 ms below the picked horizon through ten spectral magnitude and phase components at 10 Hz increments corendered using a 2D color wheel. Grayer levels indicate lower spectral magnitude. The white and yellow arrows show some of the lineaments in orthogonal directions that stand out.

Principal component analysis

When it comes to the analysis of a large number of seismic attributes, principal component analysis comes in as a handy tool to 'churn' through the different attributes and come up with a fewer number (say 2) of attributes which can be interpreted easily. The choice of the attributes that have to be chosen for the principal component analysis would of course be dependent on the goal of the exercise that has to be performed. For the applications mentioned above, the work carried out by Tingdahl and Hemstra (2003) focused on the fault orientations, and so the choice of the attributes input into the exercise were all that had some kind of definition of the faults. The facies determination exercise by Singh (2007) used the AVO attributes, but since the fluid discrimination was the objective, the PC2 component was more forthcoming in yielding good results. Spectral components analysis done by Guo et al. (2009) used spectral magnitude volumes to compute a suite of "eigenspectra". Guo et al. (2009) prototyped, and Wallet (2014) applied complex principal component analysis to a suite of complex (magnitude, r, and phase, φ) components, $U(f,x,y)=r(f,x,y)exp[-j\varphi(f,x,y)]$ resulting in complex (magnitude and phase) principal components. We followed this approach and carried out principal component analysis on spectral magnitude and phase components with frequencies 30, 40, 50, 60, 70 and 80 Hz. By construction, the first principal component was found to have contributed much more than the second or the lower ones and we used that for interpretation.

In Figure 4 we show phantom horizon slices below the picked horizon through the first four complex spectral principal components obtained by projecting the complex data spectra onto the first four complex eigenspectra. The magnitude and phase are displayed against saturation and hue as in the previous figure and co-rendered with coherence displayed against lightness. We notice that the first eigenspectra best represents the variation within the data (Figure 4b). In Figure 4c we also show the equivalent phantom horizon slice through the coherence volume, to show that the discontinuities in phase are helpful in delineating the faults.

Conclusions

We demonstrate the performance of the traditional phase attribute generated using complex trace analysis and compare it with the phase components that can be generated at different frequencies via spectral decomposition. The motivation for doing this comes from the fact that spectral decomposition allows the generation and analysis of amplitude and phase spectra of seismic data. Besides the amplitude spectra which are normally studied, the phase attribute can be studied in a frequency-dependent way, such that the subsurface geologic features can be visualized at different frequencies.

We found that of the CWT and the MP methods for carrying out spectral decomposition, the MP method yields crisper definition of the geologic features. Instead of visualizing the spectral phase components at different frequencies, we utilized the principal component analysis to reduce the dimensionality of these attributes.

Analysis of the complex spectral principal components generated from the spectral and phase components at different frequencies and increments, can show sharper definition of the subsurface features, which improves their interpretability.

Acknowledgements

We wish to thank Arcis Seismic Solutions, TGS, Calgary, Canada for encouraging this work and for permission to present these results.

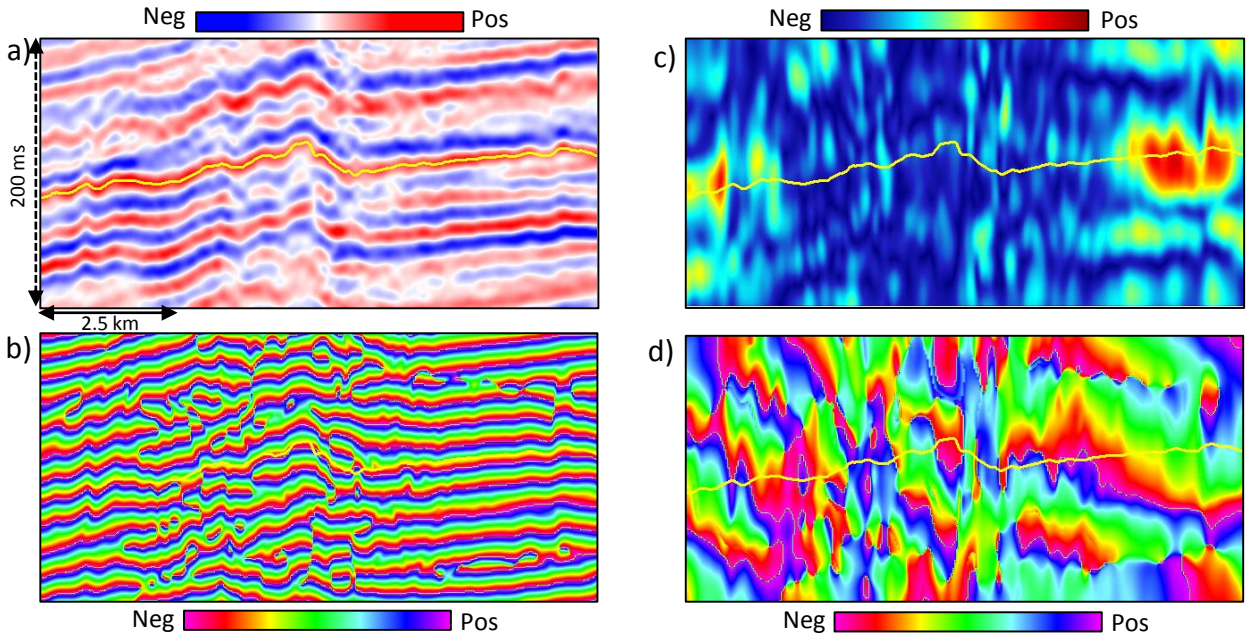

Figure 1: (a) A segment of a seismic section, (b) Equivalent sections from instantaneous phase, (c) 70 Hz spectral magnitude component, and (d) 70 Hz phase component. *Data courtesy: Arcis Seismic Solutions, TGS)*

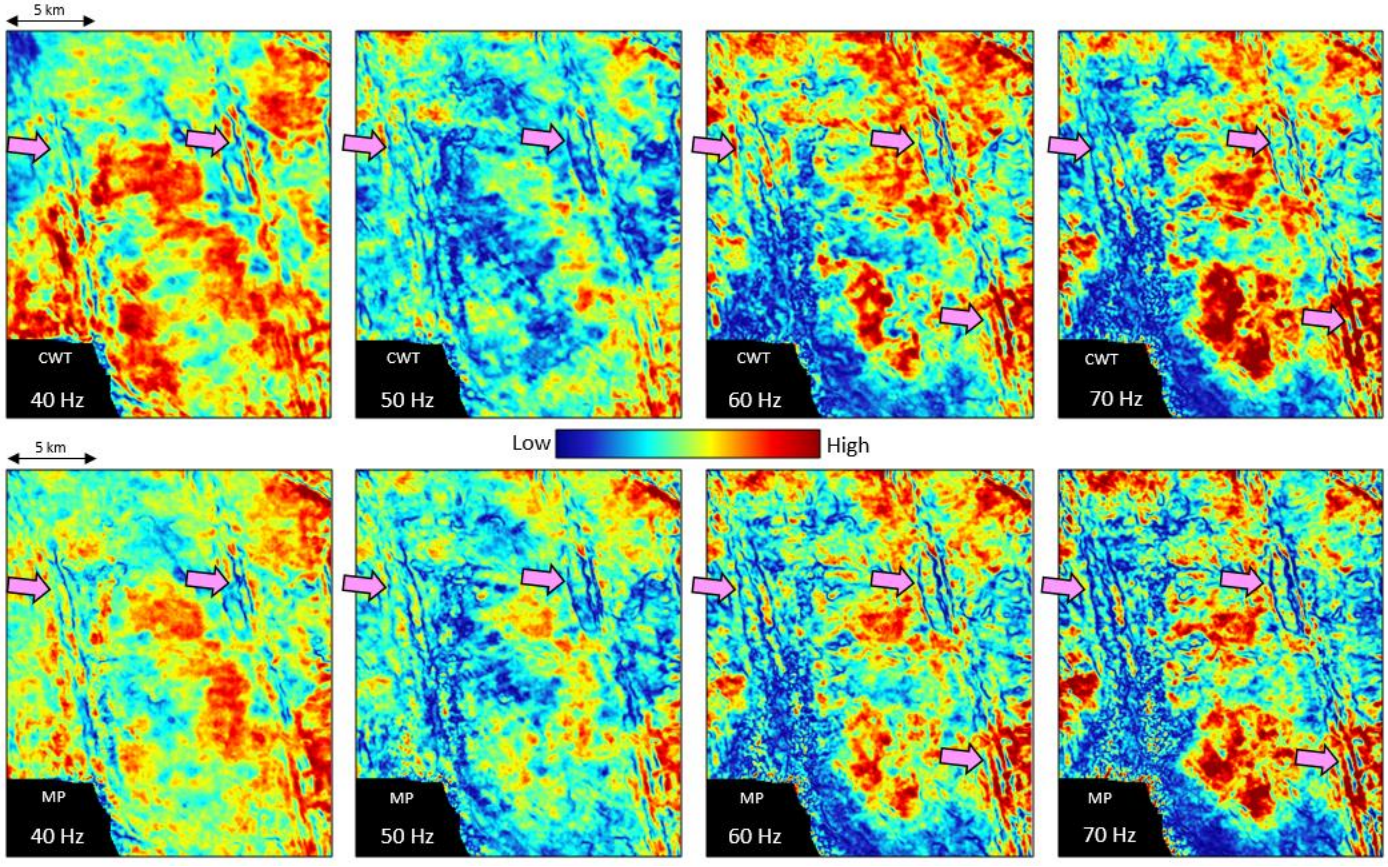

Figure 2: Stratal slice 8 ms below the yellow horizon marked in Figure 1 from the spectral magnitude using (above) the continuous wavelet transform (CWT) method, and (below) matching pursuit (MP) method at different frequencies indicated on the images. On comparing, one can notice the sharper definition of the NW-SE discontinuity events on the MP displays, as indicated with the pink arrows. Some E-W events are also seen on both displays, but sharper on the MP displays. *Data courtesy: Arcis Seismic Solutions, TGS)*

DOI http://dx.doi.org/10.1190/segam2015-5874263.1

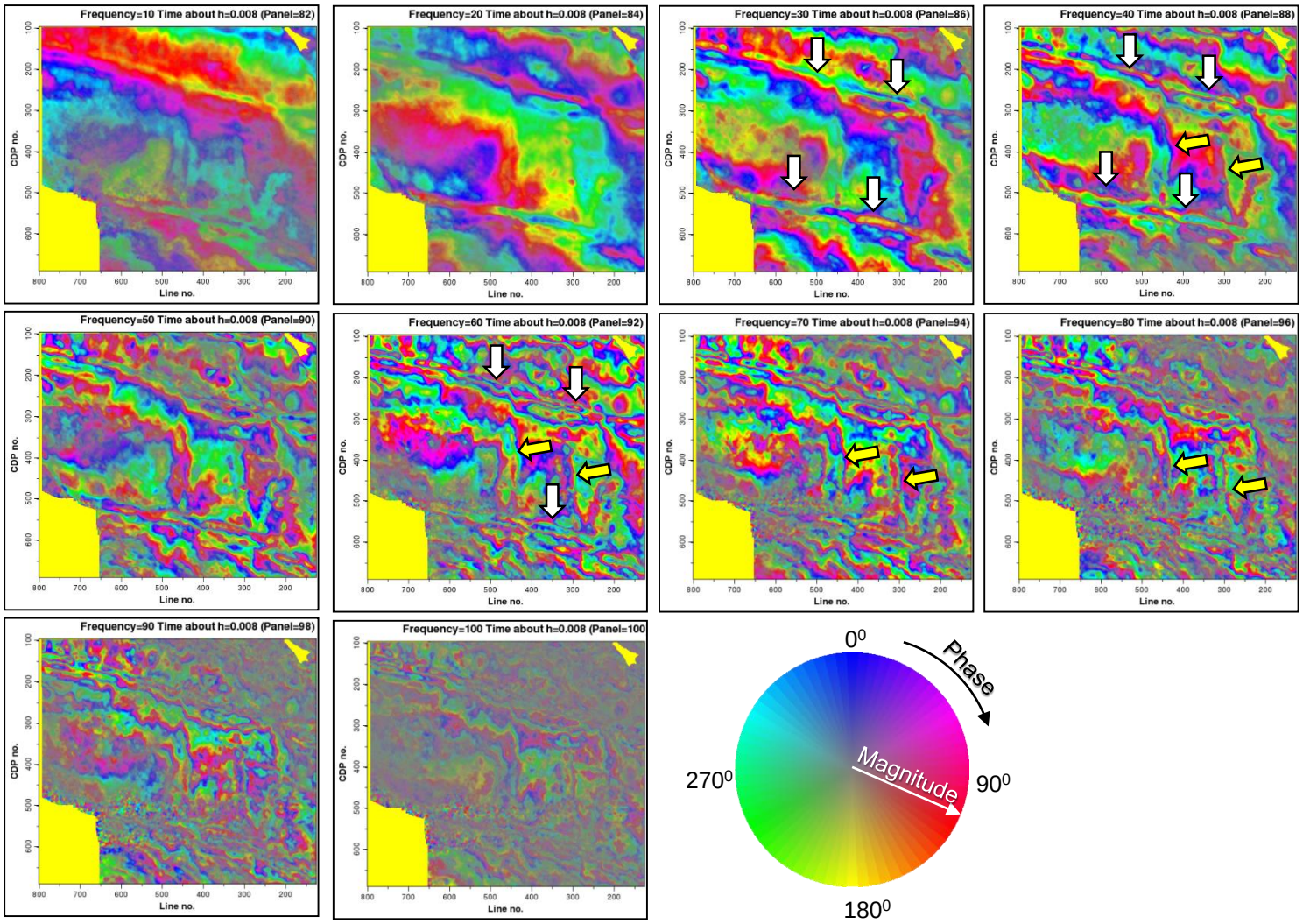

Figure 3: Phantom horizon slice 8 ms below the picked horizon through ten spectral magnitude and phase components at 10 Hz increments corendered using a 2D color wheel. Grayer levels indicated lower spectral magnitude. The spectral components have been balanced to provide a relatively flat spectrum when averaged for the entire survey. *(Data courtesy: Arcis Seismic Solutions, TGS)*

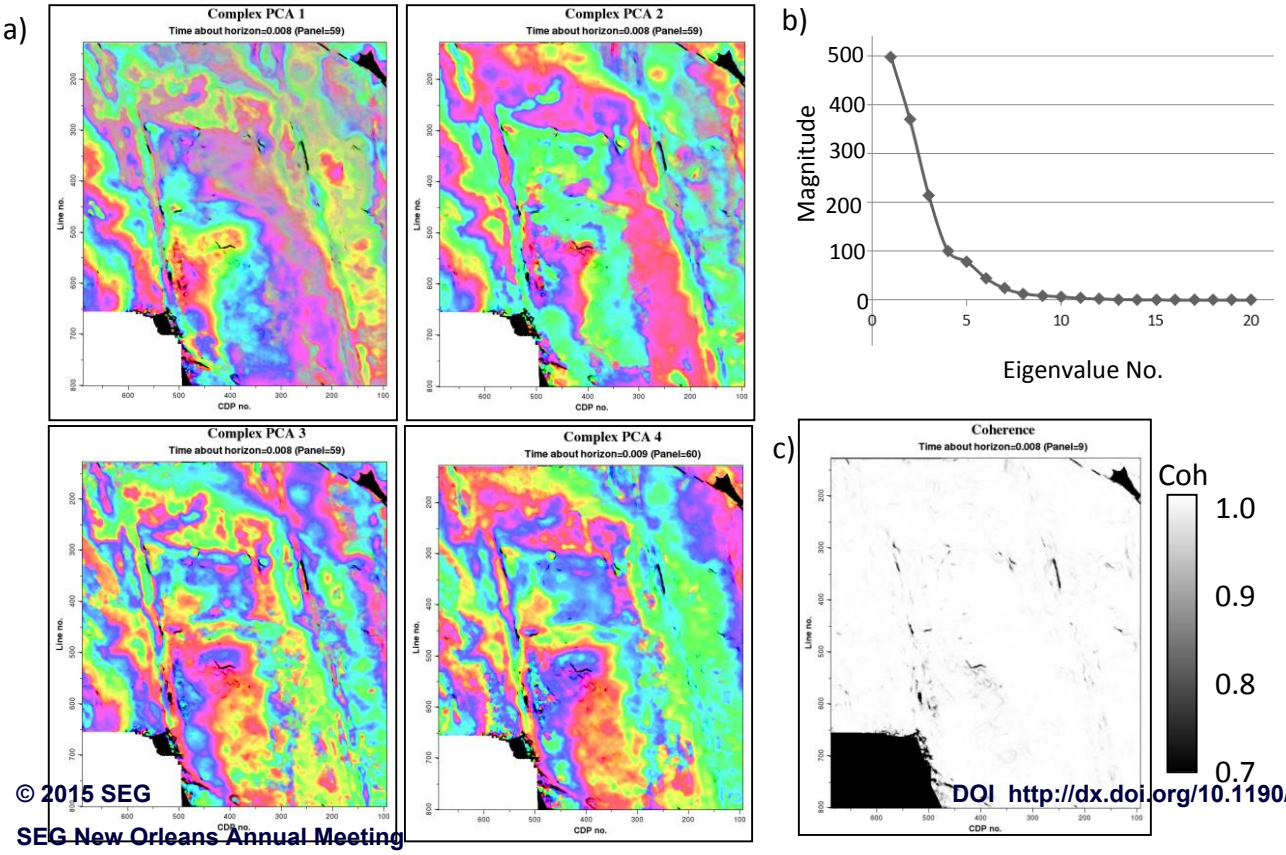

Figure 4. (a) Phantom horizon slices 8 ms below the picked horizon through the first four complex spectral principal components obtained by projecting the complex data spectra projected onto the first four complex eigenspectra. (b) By construction, the first eigenspectra best represents the variation within the data. The magnitude and phase are displayed against saturation and hue as in the previous figure and co-rendered with coherence displayed against lightness. (c) The equivalent phantom horizon slice through the coherence volume by itself. Note how the discontinuities in phase help delineate the faults. *(Data courtesy: Arcis Seismic Solutions, TGS)*

DOI http://dx.doi.org/10.1190/segam2015-5874263.1

EDITED REFERENCES

Note: This reference list is a copyedited version of the reference list submitted by the author. Reference lists for the 2015 SEG Technical Program Expanded Abstracts have been copyedited so that references provided with the online metadata for each paper will achieve a high degree of linking to cited sources that appear on the Web.

REFERENCES

Chopra, S., and K. J. Marfurt, 2014, Churning seismic attributes with principal component analysis: 82nd Annual International Meeting, SEG, Expanded Abstracts, 2672–2676.

Chopra, S., and K. J. Marfurt, 2015, Choice of mother wavelets in CWT spectral decomposition: Presented at the 83rd Annual International Meeting, SEG.

Guo, H., K. Marfurt, and J. Liu, 2009, Principal component spectral analysis: Geophysics, **74**, no. 4, P35–P43. http://dx.doi.org/10.1190/1.3119264.

Liu, J. L., and K. J. Marfurt, 2007, Multicolor display of spectral attributes: The Leading Edge, **26**, 268–271. http://dx.doi.org/10.1190/1.2715047.

Mallat, S., and Z. Zhang, 1993, Matching pursuits with time-frequency dictionaries: IEEE Transactions on Signal Processing, **41**, no. 12, 3397–3415. http://dx.doi.org/10.1109/78.258082.

Partyka, G. A., J. M. Gridley, and J. Lopez, 1999, Interpretational applications of spectral decomposition in reservoir characterization: The Leading Edge, **18**, 353–360. http://dx.doi.org/10.1190/1.1438295.

Singh, Y., 2007, Lithofacies detection through simultaneous inversion and principal component attributes: The Leading Edge, **26**, 1568–1575. http://dx.doi.org/10.1190/1.2821944.

Sinha, S., P. S. Routh, P. D. Anno, and J. P. Castagna, 2005, Spectral decomposition of seismic data with continuous-wavelet transform: Geophysics, **70**, no. 6, P19–P25. http://dx.doi.org/10.1190/1.2127113.

Stockwell, R. G., L. Mansinha, and R. P. Lowe, 1996, Localization of the complex spectrum: The S-transform: IEEE Transactions on Signal Processing, **44**, no. 4, 998–1001. http://dx.doi.org/10.1109/78.492555.

Taner, M. T., F. Koehler, and R. E. Sheriff, 1979, Complex seismic trace analysis: Geophysics, **44**, 1041–1063. http://dx.doi.org/10.1190/1.1440994.

Tingdahl, K., and N. Hemstra, 2003, Estimating fault-attribute orientation with gradient analysis, principal component analysis and the localized Hough-transform: 71st Annual International Meeting, SEG, Expanded Abstracts, 358–361.

Wallet, B., 2014, Seismic attribute expression of fluvial-deltaic and turbidite systems: Ph.D. dissertation, The University of Oklahoma.